Magnetocapacitance of quantum wires: Effect of confining potential on one-dimensional subbands and suppression of exchange enhanced *g* factor

I. Pallecchi,[1,2,*] Ch. Heyn,[1] J. Lohse,[1] B. Kramer,[3] and W. Hansen[1]
[1]*Institut für Angewandte Physik, Universität Hamburg, Jungiusstraße 11, D-20355 Hamburg, Germany*
[2]*I.N.F.M., Dipartimento di Fisica, Via Dodecaneso 33, I-16146 Genova, Italy*
[3]*Institut für Theoretische Physik, Universität Hamburg, Jungiusstraße 11, D-20355 Hamburg, Germany*
(Received 29 August 2001; published 1 March 2002)

By means of magnetocapacitance measurements, we study subband filling in field effect induced arrays of quantum wires in GaAs/AlGaAs heterostructures. The confining potential is defined by fork-shaped interdigitated metallic gates with lithographic width of ~150 nm, realized by *e*-beam lithography. The capacitance allows us to investigate the density of states. Evolution of one-dimensional subband spacing and filling as a function of confinement, gate voltage and magnetic field is analyzed and quantitatively explained. Also the development of a structure related to spin splitting is studied as a function of both magnetic field and confinement. In different regimes, we find for the *g* factor either an enhancement up to a factor of almost 50 with respect to the ''bare'' value or a suppression, accounting for exchange interactions and kinetic energy of edge electrons, respectively, in agreement with theoretical models.

DOI: 10.1103/PhysRevB.65.125303 PACS number(s): 71.70.Gm, 73.21.Hb, 73.40.Qv, 71.70.Ej

I. INTRODUCTION

Electron systems of reduced dimensionality exhibit a wide range of phenomena related to many-body effects and electrons interactions. The Landé *g* factor, describing lifting of spin degeneracy in presence of a magnetic field B as $\Delta E_{\mathrm{spin}}=g\mu_B B$, where ΔE_{spin} the spin gap and μ_B the Bohr magneton, is strongly affected by electron interactions, which become more important as the dimensionality of the system is lowered from two to one. In the pioneering work of Fang and Stiles,[1] it has been experimentally found for the first time that the *g* factor in a silicon inversion layer is enhanced with respect to the bulk value and it is dependent on the electron density. Janak[2] has first explained such behavior in terms of exchange interactions, which are enhanced whenever the populations of spin split levels are different. The effect is made plausible with a simple picture, considering the Coulomb repulsion among the electrons in the many-particle states associated to the different spin systems. The Pauli exclusion principle enforces larger average distances of electrons carrying the same spin, compared to those with different spins. Thus, due to Coulomb repulsion, many-particle states with electrons of the same spin are energetically favorable. Ando and Uemura have further clarified the theoretical picture in their celebrated work,[3] explaining the oscillatory behavior of the *g* factor as a function of filling factor in a two-dimensional (2D) system; since the enhancement depends directly on the population difference of the spin split pair of the same Landau level (LL), it is maximum when the Fermi level lies in the spin gap between the levels themselves and it approaches a minimum value close to the ''bare'' value, when the Fermi level lies midway between spin states originating from different Landau levels. This picture has been confirmed by a number of different experimental methods, such as measurements of activation energies in magnetotransport,[4,5] direct spectroscopic measurements by inelastic light scattering,[6] magnetization,[7] magneto-capacitance,[8] and optical absorption spectroscopy.[9] In all cases, significant enhancements have been found with respect to the bulk value, that for GaAs is $g\sim-0.44$.[10] Reported values are between 1 and 10. Additional corrections to the bulk *g* factor in two dimensions other than exchange interactions have also been suggested, either intrinsically related to quantum confinement[11] or to asymmetric interface potentials and interaction between different subbands.[12] To describe the spin gap in spin polarized quantum Hall states, elementary charge excitations consisting of spin textures, known as Skyrmions, have been theoretically predicted in GaAs systems[13] as well as experimentally observed.[14,15]

In one-dimensional (1D) systems, where interactions have an even more dramatic effect, altering completely the shape of ground state and Fermi surface, one could naively expect this enhancement to be more pronounced, but this would be an oversimplified conclusion. Indeed, theoretical as well as experimental scenarios are far more complicated and controversial and it seems that opposite behaviors should be expected in different regimes. Let us first discuss the situation where the magnetic field is applied in the direction of strongest confinement, i.e., perpendicular to the plane of the two-dimensional electron gas (2DEG) out of which the wires are generally prepared. In our experiment the magnetic field is oriented in this direction. Confinement of a 2DEG to lower dimension is predicted by Kinaret and Lee[16] to suppress the spin splitting in high magnetic field. A further refined model has been proposed by Balev and Vasilopoulos,[17] who have treated exchange and correlations self-consistently, beyond the Hartree-Fock approximation. They have deduced a suppression of spin splitting, accounted for in terms of correlation effects and spatially inhomogeneous screening, in the strong magnetic field limit $e^2/4\pi\varepsilon_0\varepsilon_r l_0\hbar\omega_c \ll 1$, $\omega_c/\omega_0 \gg 1$, where $l_0=\sqrt{\hbar/eB}$ is the magnetic length, $\omega_c=eB/m^*$ the cyclotron frequency, and ω_0 describing the curvature of the parabolic confining potential $\frac{1}{2}m^*\omega_0^2x^2$. On the other hand the opposite trend has been suggested by Shepard,[18]

who has predicted a strengthening of the electron-electron interactions by interactions with polarizable edge-state charges, in a regime reached in wires of somewhat larger width than those considered by Kinaret and Lee. Spin splitting suppression has been observed experimentally by Wróbel[19] in magnetotransport measurements in quasiballistic GaAs/AlGaAs quantum wires, as well as by Kastner[20] and Mottahedeh[21] in narrow silicon inversion layers. On the contrary, exchange enhancement with decreasing width of the wire has been measured by Shepard[18] in support of his theoretical description. Also Kotlyar and co-workers[22] have recently presented a systematic theoretical and experimental study of spin splitting in semiconductor nanostructures in a perpendicular magnetic field. By photoluminescence spectra in quantum wires, they have extracted an enhanced g factor, which increases from the bulk value up to $|g|\approx 5$ with decreasing wire width, and they have accounted for their experimental findings by means of a six-band effective-mass perturbative calculation. In split gate devices with ballistic 1D channels, so-called quantum point contacts, features have been observed in the conductance data near $0.72e^2/\hbar$, in the absence of any magnetic field. They have been discussed in terms of spontaneous polarization,[23–25] which would be in accordance with the predictions of enhanced exchange effects in quantum wires.[26–28] The quantum point contacts have been investigated in parallel magnetic field. An enhanced g factor is observed. It is reported to be $|g|\approx 1.3$ when only a few subbands are occupied, while it saturates to a value close to the bulk limit with increasing subband index.[29,30] On long wire systems, an in-plane magnetic field has been found not to induce spin related structures up to fields of 20 T.[31]

In this paper we present capacitance measurements performed on quantum wires induced by field effect in GaAs/AlGaAs metal-insulator-semiconductor (MIS) type heterostructures. Capacitance spectroscopy is a powerful means to investigate directly the occupation of 1D subbands.[32,33] The interdigitated electrodes allow us to tune the confining potential and the electron density independently so that we can study the behavior of wires in the quantum limit, i.e., only one single subband occupied, as a function of confinement. The paper is structured as follows. In Sec. II we describe the sample and the experimental setup; in Sec. III, we present our results and we discuss them within the framework of theoretical models; finally, we draw our conclusions in Sec. IV.

II. EXPERIMENTAL

The samples studied in this work are MIS-type AlGaAs/GaAs heterostructures, whose deposition sequence is sketched in Fig. 1(a). On a superlattice AlAs/GaAs buffer layer a highly silicon doped (2.7×10^{18} cm^{-3}) GaAs layer is deposited, which is used as ground plane for applied gate voltages. Furthermore, it serves as a back contact, i.e., it provides a charge reservoir for the low-dimensional electron system. The low dimensional system under study (called ''upper'' 2DEG in the following) is generated at the interface

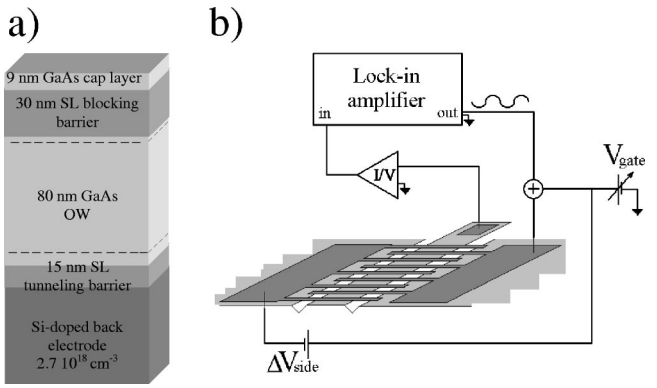

FIG. 1. (a) Deposition sequence of MBE grown AlGaAS/GaAs heterostructure; (b) circuit diagram of the measurement.

between a 80 nm thick GaAs layer and a 25 nm thick AlAs/GaAs superlattice blocking barrier, when the gate electrode at the surface is biased with a positive voltage, larger than a certain threshold value. An additional tunneling barrier is placed just above the back contact. The latter causes the formation of a second 2DEG (called ''lower'' 2DEG in the following) at the bottom end of the 80 nm quantum well. The tunneling barrier, which was introduced in order to study the tunnel coupling between the 2DEG and the wires, plays no role in the effects discussed in the following. Finally, the structure is capped with a 9 nm thick GaAs layer. The top gate electrode is fabricated by high resolution electron beam lithography, using a bilayer PMMA resist. It consists of a 30 nm thick titanium layer, shaped as a pair of interlocked forks, whose 22 fingers are stripes of nearly 150 nm lithographic width and 56 μm length, corresponding to a total length of 1.25 mm. The resulting potential modulation has a 540 nm period. As such modulation decays exponentially with the distance from the surface, the front barrier between electron system and gate has to be kept as small as possible. In order to preserve high mobility and well defined potentials even at low carrier densities, we use undoped front barriers. One-dimensional wires are generated beneath one of the two fingergates that is biased with a positive voltage V_g, as depicted in Fig. 1(b). The other fingergate, called side gate in the following, is biased with a constant negative dc voltage V_{side}, applied with respect to V_g. Its task is to deplete the underlying region between subsequent stripes of the positively biased fingergate, allowing controlled tuning of the width as well as of the wall steepness of the potential wells where the wires are formed.

By a standard synchronous detection technique, we measure the imaginary (out-of-phase) and real (in-phase) parts of the ac current flowing from the back contact to the front electrode. The circuit configuration is sketched in Fig. 1(b). From the output signal we extract the differential capacitance dQ/dV_g and the tunneling resistance of our sample. We employ an excitation voltage of 1 mV amplitude and 40 kHz frequency superimposed to a dc voltage sweep of V_g. The measurements are performed in a dilution cryostat at bath temperatures of few tens of mK.

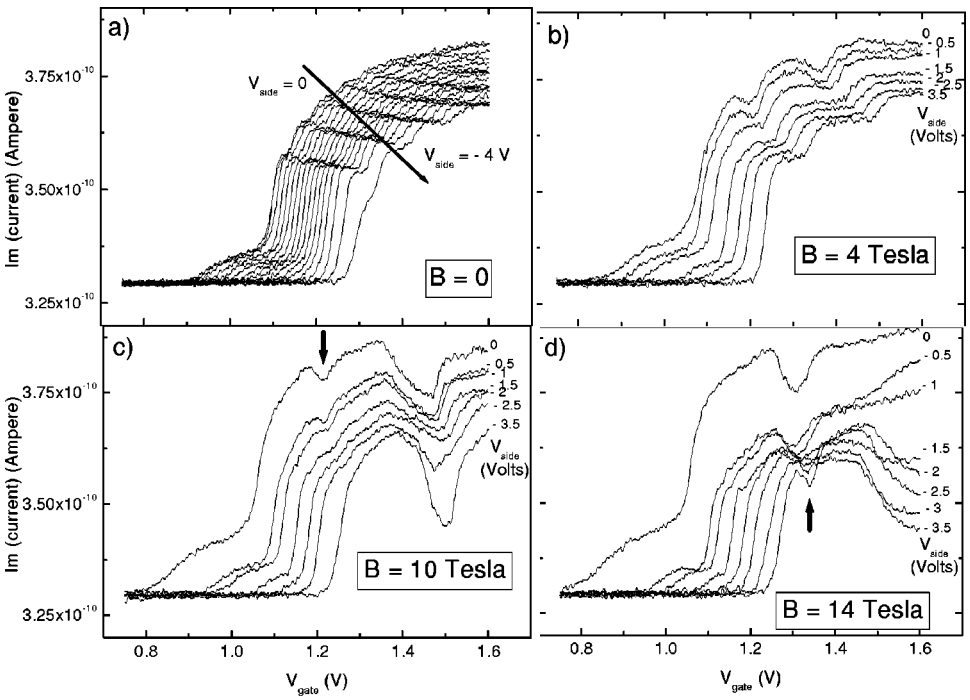

FIG. 2. Traces of the 900-out-of-phase part of the current versus dc gate voltage at some selected values of magnetic field and side gate voltage indicated in the figure. The curves in (a) are measured with V_{side} from 0 to -4 V in steps of -0.25 V. In all cases, an excitation voltage of 1 mV amplitude and a frequency of 40 kHz are used. The arrows in (c) and (d) indicate spin splitting minima.

III. RESULTS AND DISCUSSION

A. Capacitance and density of states

As long as the charge exchange between back gate and electron system is quick enough with respect to the period of the excitation, the real part of the signal is nearly two orders of magnitude smaller than the imaginary part, featureless and almost constant over the whole range of V_g up to 1.6 V, beyond which breakdown leakage current onsets. In these conditions, the imaginary signal is directly related to the differential capacitance, briefly indicated as capacitance in the following. Instead, with increasingly negative V_{side}, a regime is reached in which tunneling begins to be hampered: broad peaks in the real part rise at the onset of 1D subbands and, correspondingly, the imaginary part decreases and does no longer reflect the device capacitance alone. The value of V_{side} which marks the crossing between these two regimes depends on the magnetic field applied perpendicularly to the sample surface. In the following, we avoid making quantitative analysis of the imaginary signal, whenever any not negligible feature in the corresponding real part is present.

In Figs. 2(a)–2(d), traces of the capacitance of the wire array as a function of V_g for different confinements and magnetic fields are presented. At small V_g the measured capacitance is the one between top and back electrodes plus other stray contributions originating from the experimental setup and from the sample itself. At characteristic threshold voltages the lower and upper electron systems start forming, which in the measured signal is accompanied by a corresponding sharp rise of the capacitance. A first, relatively small step reflects the formation of the lower electron system. The corresponding threshold voltages monotonously increase from 0.9 V on with increasing value of the side gate bias. A second, much stronger rise marks the threshold voltage of the upper electron system. We note that the capacitance between the two threshold voltages is featureless and almost constant. The distance between the threshold voltages decreases with increasing side gate bias indicating that the lower electron system more sensitively reacts on the side gates than the upper system. Above behavior can be well reproduced in simulations of the capacitance with a self-consistent Poisson solver. There the lower electron system arises if we allow for diffusion of some n dopants from the back contact to the tunnel barrier. The threshold voltage of the upper system shifts from 1.08 to 1.28 V as V_{side} is varied between 0 and -4 V. Beyond the threshold, the measured signal then reflects essentially the capacitance between the front gate and the low dimensional system closest to the front gate. Pronounced steps are visible in the capacitance of the upper system, superimposed to a slow continuous rise of the signal. These steps establish that the upper system consists of 1D quantum wires. The height, width and slope of the steps depend on the side gate voltage and mark the onset of successive 1D subbands.[33] Indeed, because of the finite density of states (DOS), the electric field from the top gate is not completely screened by the quantum wire; any charge increment in the electron system is then accompanied by a surface charge induced beneath the electron system, which equilibrates the chemical potential of the whole system, whereas the Fermi level of the low dimensional system rises with respect to the bottom of the conduction band. In a simple picture, the capacitance of system can be thought of as resulting mainly from two contributions: a geometrical one C_{geo}, corresponding to ideal metallic electrodes placed at the top gate and at the low dimensional system, respectively and a contribution $C_{\mathrm{DOS}} \sim e^2 D$ arising from the finite density of states D of the low dimensional system. From the set of traces at zero field it can be seen that, at equal filling factor, the average signal drops slightly as the confinement increases, due to the fact that the wire width shrinks with

increasing confinement. In addition, at high magnetic field ($B \gtrsim 10$ T), the imaginary signal is significantly reduced with increasing confinement, due to the not negligible increase in the tunneling resistance. In such regime, a simple relation between imaginary current and capacitance cannot be extracted and no quantitative analysis of the absolute value of the capacitance is attempted.

Above a certain magnetic field, that is nearly 7 T for the lowest confinement and higher for higher confinement, structures related to spin splitting of the first hybrid subband, indicated by arrows in Figs. 2(c) and 2(d), start to develop. Such structures, which are the central issue of this paper and will be discussed later on in detail, are not accompanied by any related feature in the real part of the signal.

In order to get a slightly more quantitative idea of the effect of the side gate voltage, we can assume that the confining potential and the wire capacitance C_{wire} are roughly constant throughout the filling of the first subband and can be approximated by their mean value. Furthermore, we assume for simplicity that the confining potential is parabolic $\frac{1}{2}m^*\omega_0^2x^2$ and that the density of states is the ideal 1D single particle DOS, neglecting broadening and many-particle effects. In this simple picture, the total number of electrons per unit length n_{ql} that can be placed in the first subband is easily obtained by integration of the 1D density of states over the first subband, that yields

$$n_{ql}=\int_0^{\hbar\omega}\frac{\omega}{\omega_0}\frac{2}{\pi\hbar}\sqrt{\frac{m^*}{2E}}dE=\sqrt{\frac{8m^*}{\pi^2\hbar}}\frac{(\omega_0^2+\omega_c^2)^{3/4}}{\omega_0}, \quad (1)$$

where $\omega=\sqrt{\omega_0^2+\omega_c^2}$. After defining the wire capacitance C_{wire} in terms of the gate voltage U_{ql} at which the second subband starts to be filled, as

$$en_{ql}=C_{\mathrm{wire}}U_{ql} \quad (2)$$

it follows that a linear relation can be established between squared magnetic field B^2 and $U_{ql}^{4/3}$:

$$U_{ql}^{4/3}=a_0+a_1B^2, \quad (3)$$

where we define

$$a_0=\left(\frac{\alpha e}{C_{\mathrm{wire}}}\right)^{4/3}\omega_0^{2/3}, \quad a_1=\left(\frac{\alpha e}{C_{\mathrm{wire}}\omega_0}\right)^{4/3}\left(\frac{e}{m^*}\right)^2,$$

$$\text{and} \quad \alpha=\frac{2}{\pi}\sqrt{\frac{m^*}{\hbar}}. \quad (4)$$

For the second subband the same equations for a_0 and a_1 are still valid, but defining $\alpha=4/\pi\sqrt{m^*/\hbar}$. From a set of curves measured at the same V_{side} and at different magnetic fields, one can obtain the measured values for the plot $U_{ql}^{4/3}$ versus B^2, as shown in Fig. 3, and extract the experimental values for C_{wire} and ω_0. Of course, the slope of the trace superimposed to the capacitance steps tells us that actually the geometric capacitance increases all the time as the system is filled, because of widening of the wires due to Coulomb repulsion. Additionally, at very low densities, many-particle effects are likely to affect the potential shape and, accordingly, also the subband spacing and the wire capacitance.[32] Yet, the linear relation between the data points is an *a posteriori* check that our assumption is not too bad. Moreover, a direct comparison of our values of subband occupation and energy levels with those computed by means of the self-consistent Poisson-Schrödinger calculation developed by Schmerek,[32] based on spin dependent local density approximation, shows that the numerical and analytical approaches are in very good quantitative agreement. For a detailed description of the calculation we refer to Refs. 34,32. It is apparent from Fig. 3 that the electron density n_{ql} is less affected by a magnetic field if the confinement is strong. This is in agreement with Eq. (4) predicting a linear relation between B^2 and $U_{ql}^{4/3}$. Since at zero field n_{ql} increases with the confinement, this implies that the behavior of n_{ql} as function of the side gate voltage reverses at high fields. This can be clearly seen in the inset of Fig. 3: at low fields ($B<2$ T) n_{ql} increases with side gate voltage, whereas it decreases at high fields ($B>3$ T). The physical explanation for this crossover can be understood on basis of Eqs. (1) and (2). At zero magnetic field the 1D confinement rules the density of states leading to high state densities close to the subband edge. Similar to the subband spacing, n_{ql} is increasing with confinement. It is well known that at zero confinement and high magnetic fields the state density condenses into discrete and highly degenerate LL. Here the 1D confinement counteracts leading to hybrid subbands with dispersion and thus to a redistribution of state density to higher energies. On the other hand, at high field $\omega_c \gg \omega_0$ the subband spacing increases very slowly with ω_0, being mostly determined by the magnetic field itself. Thus, in high magnetic fields, n_{ql} decreases with increasing confinement.

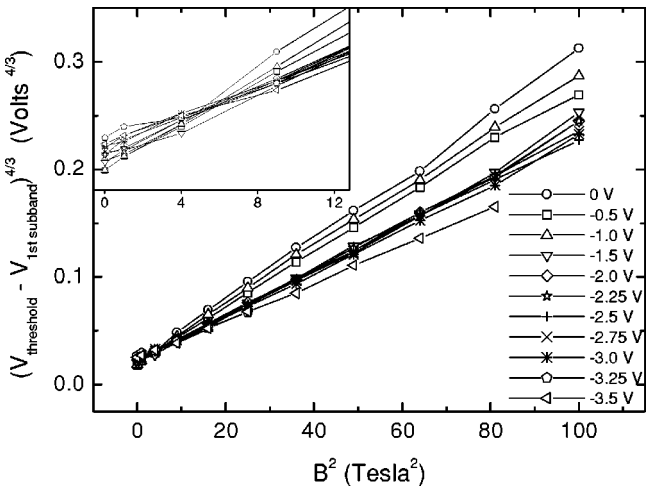

FIG. 3. Plot of $U_{ql}^{4/3}$ versus squared magnetic field B^2, extracted form experimental curves of the imaginary part of the current, as explained in the text. Side gate voltage values V_{side} are indicated in the legend. The lines connecting data points are guides to the eyes. In the inset, the low magnetic field region where the curves cross is expanded.

In Figs. 4(a) and 4(b) the values for ω_0 and C_{wire} resulting from this fitting procedure are plotted as a function of the confinement for the first and the second 1D subbands, with the corresponding uncertainties. The capacitance C_{wire} is

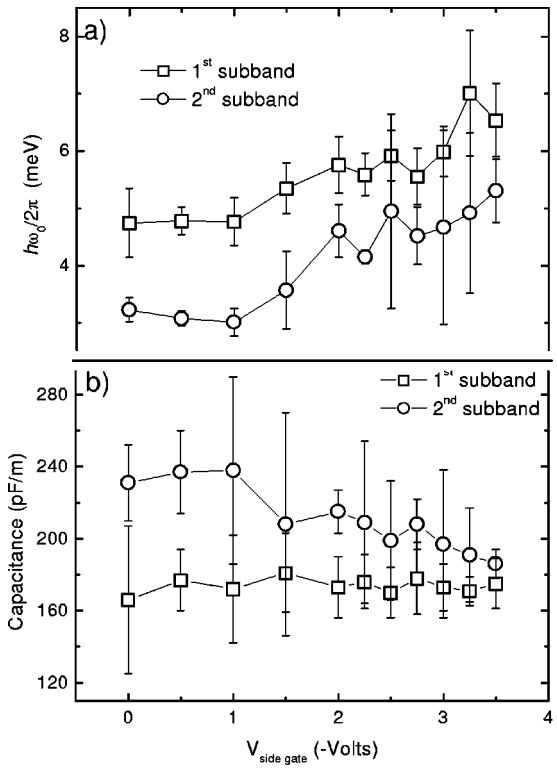

FIG. 4. (a) 1D subband spacing and (b) wire capacitance C_{wire} extracted from the linear fit of data points in Fig. 3 as a function of the side gate voltage.

nearly constant in the whole range of V_{side} values. The subband spacing, as expected, slowly increases with increasingly negative side gate voltage, being for the first subband $\hbar\omega_0 \approx 4.75$ meV at $V_{\mathrm{side}}=0$ and $\hbar\omega_0 \approx 6.54$ meV at $V_{\mathrm{side}}=-3.5$ V. The gate voltage $V_{\mathrm{side}}=-3.5$ V is the maximum confinement at which we apply this analysis, as, beyond this value, a peak in the resistive part rises, indicating that reequilibration upon tunneling is not anymore able to follow the ac excitation and the system is no longer charged efficiently. This is clearly seen in Fig. 2(a), where the highest confinement trace significantly drops compared to the other traces. One may be surprised that the case $V_{\mathrm{side}}=0$ yields a finite ω_0, instead of approaching the 2D limit $\omega_0 \rightarrow 0$. This is probably due to surface charges localized between adjacent titanium stripes, which cause a modulation of the potential even at zero bias. This hypothesis is also supported by the observation that for $|V_{\mathrm{side}}| \leqslant 1$ V, the resulting subband spacing does not change appreciably, indicating that surface charges generate an effective electric field stronger than that generated by the side gate. Therefore, such charges, whose density is unknown and sometimes even not constant in time, introduce an additional uncertainty on the relationship between side gate voltage and effective confinement for $|V_{\mathrm{side}}| \leqslant 1$ V. Accordingly, the self-consistent Schrödinger-Poisson solver reproduces experimental data if homogeneous negative surface charge with density -3.1×10^{16} m^{-2}, as well as 12 nm wide stripes of positive surface charge with density $+1.0\times10^{17}$ m^{-2} beside the gate electrodes are assumed. The subband spacing and the capacitance of the second subband are, respectively, systematically lower and larger than those of the first subband, as expected from an effective confining potential shape that is flattened and broadened by screening, as the electron density increases.[35,36]

A comparison of the traces of Figs. 2(b)–2(d) evidences that the shape of the minima associated to 1D subbands changes with both magnetic field and confining voltage. At small magnetic field ($B<4$ T) the rather symmetric minima evolve into plateauxlike steps as confinement increases. At high field ($B>8$ T) the LL minima at low confinement appear to be asymmetric with a smoother fall and a steeper rise, while they become clearly deeper and more symmetric at the largest confinements. We suggest that the behavior at low field [Fig. 2(b)] mirrors the character of the 1D density of states: at low confinement the shape of hybrid levels is reminiscent of the shape of Landau levels and the capacitance shape is closer to a typical 2DEG capacitance trace (see, for example, Ref. 37). At high confinement, the decrease of the tail of each hybrid level DOS is expected to be slower as compared to that of a LL, so that also the decrease of the capacitance as the subband is filled is slower. Actually there is almost no decrease at all, but rather a constant plateau before the onset of the subsequent subband. We believe that this vanishing slope comes out from the fortuitous compensation of the rising geometrical term C_{geo} and the density of states term C_{DOS}. At higher field, the larger subband spacing results in an enhanced sensitivity of the measurement along the gate voltage axis, therefore, at low confinement, the 1D character of the density of states becomes more and more visible. The slow fall and the steep rise around each LL minimum [Fig. 2(c)] mirror the square root fall of the density of states of each subband and the abrupt rise of the DOS of the subsequent subband, respectively. At the highest confinements -3.5 V$\leqslant V_{\mathrm{side}} \leqslant -2.5$ V, the shapes of the traces are affected by the increase of the tunneling resistance and the LL minima are made symmetrically deeper in correspondence to a broad rising peak in the real part. Indeed, a comparative observation of the evolution of the resistance peaks and of the shape of the capacitance minima with varying magnetic field and confinement supports this interpretation.

B. The *g* factor

We would like to discuss now the behavior of the spin splitting. As it can be seen in Figs. 2(c)–2(d), contrarily to the 2D case, where the spin splitting minima occur at a gate voltage that is exactly halfway between two adjacent LL minima, in this case it is shifted to lower voltages. This trend becomes more and more evident with increasing confinement and can be explained qualitatively in terms of the asymmetric shape of the 1D density of states. Another even more evident effect is that with increasing confinement, the spin splitting feature is blurred out: at magnetic fields lower than 10 T, the spin feature fades out completely as the confining potential is varied from 0 to -3.5 V. We apply to our case the model formulated by Kinaret and Lee[16] for suppression of spin splitting in 1D systems. If correlations are neglected, the total energy of the system E_{tot} as a function of electron den-

sity and magnetic field can be expressed as a sum of a positive kinetic term associated with skipping electrons in edge states, plus a negative exchange term, plus a Zeeman term. At each fixed magnetic field and confinement, a critical density n_{cr} is found, marking the crossover between two different regimes: for lower densities the exchange contribution dominates ($E_{tot}<0$) and the spin split phase is stable; above, the positive kinetic contribution suppresses the exchange related spin gap enhancement ($E_{tot}>0$) and the spin split phase is no longer stable. In other words, this can be seen as an effect of the confinement, which lifts the degeneracy of Landau levels and thus makes the exchange interaction less effective. Equivalently, at fixed electron density, a critical field B_{cr} exists, beyond which the spin split phase is stable. At an electron density of 8.5×10^{7} m^{-1}, we calculate by Eqs. (12) and (13) of Ref. 16 a critical field $B_{cr}\sim5$ T for $\hbar\omega_0\sim5$ meV confinement and $B_{cr}\sim9$ T for $\hbar\omega_0\sim7$ meV confinement. Despite the simplicity of this analytical model, these values seem to fit our experimental findings very well.

Another possible scenario to describe suppression of spin splitting in our sample may be the one proposed by Balev and Vasilopoulos.[17] They self-consistently treated exchange and correlation in a quantum wire within a modified local density approximation and found that electron correlation plus inhomogeneous screening along the wire cross section lead to suppression of spin splitting. However a quantitative comparison is not straightforward and it is not clear whether their ''optical'' *g*-factor may differ from the one extracted by magnetocapacitance measurements.

In order to extract from our data the *g*-factor of our system in a simple way, we assume the two following points: first, that the ideal 1D single particle density of states approximates the actual density of states, and, secondly, that, using the constant average capacitance C_{wire} obtained by Eq. (4), the electron density n_{spin} that completely fills the lower spin subband can be related with the correspondent gate voltage U_{spin}, according to

$$n_{spin}=\frac{C_{wire}\Delta U_{spin}}{e}. \tag{5}$$

In such simplifying assumptions, the effective *g* factor can be calculated as

$$g=\frac{1}{\mu_B B}\,\frac{\omega_0^2}{(\omega_0^2+\omega_c^2)}\,\frac{\pi^2\hbar^2}{2m^*}n_{spin}^2. \tag{6}$$

Of course, we are well aware that, on one side, the geometrical capacitance may significantly vary with electron density at very low filling and, on the other side, that the ideal single particle 1D density of states is a rough approximation for the actual density of states, which is affected by the same many-particle effects responsible for the spin splitting suppression that we want to describe. In order to justify our simple approach, we have checked, for some values of side gate voltage and magnetic field, that the positions of the capacitance features, as well as the energy levels and the subband densities obtained by Eqs. (5) and (6), are reproduced well within experimental uncertainty by the self-consistent Poisson-Schrödinger calculation developed by Schmerek,[32] based on spin dependent local density approximation. A full data analysis by means of the numerical calculation has not been performed, because it is very time consuming.

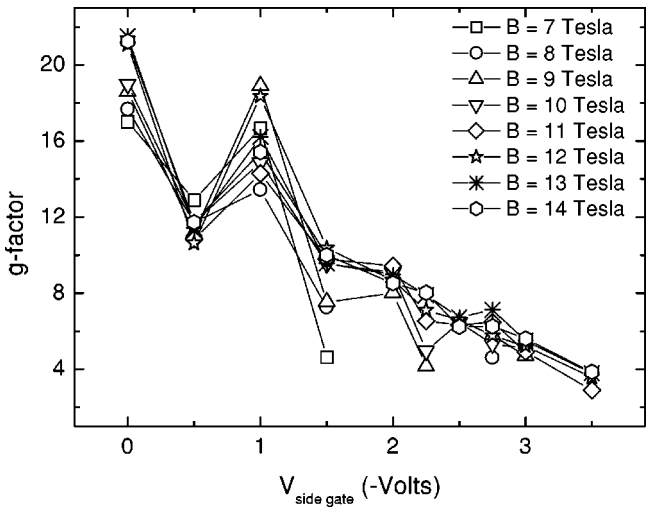

FIG. 5. Values of *g* factors extracted from the imaginary part of the measured current at different magnetic fields and confining voltages. The lines connecting data points are guides for the eyes.

In Fig. 5, we present the so obtained *g* factor of our system, as a function of confinement and magnetic field. At the weakest confinement a value $g\sim21$ at 14 T is found, that is almost 50 times larger than the ''bare'' value $g=-0.44$ and much larger than even the largest values ever found, to our knowledge, in 2D systems. The experimental uncertainty, not plotted for clarity, is estimated to be nearly 60% for the weaker confinements and 40% for the stronger ones. Such high *g*-factor values indicate that as long as the confinement is not too large, the exchange enhancement is considerable. At the same magnetic field and the highest confinement, the *g*-factor is found to drop down to ~4. At lower field, the *g* factor can be extracted only for the weaker confinements, as the spin splitting feature disappears at higher confinements. Despite the scattering of the data points, a strong reduction of the *g* factor with increasing confinement is clearly visible. Both the enhancement at low confinement and the suppression with increasing confinement are predicted by the models of Kinaret and Lee[16] as well as Balev and Vasilopoulos.[17]

The *g* values determined from our data are slightly increasing with magnetic field. However, the trend is so small with respect to experimental uncertainties that it does not allow us to establish a significant deviation from a constant *g* factor. The same behavior has been also reported in Ref. 22, where it is argued that this is the case whenever the lateral confinement energies are smaller than the quantum well confinement energies and the structure size dependence dominates over the magnetic field dependence.

In summary, we argue that our experimental results are in agreement with theoretical predictions. The high values of the *g* factor found at the lowest confinement investigated are reminiscent of an enhancement of the exchange interactions in wires, with respect to the 2D case, accordingly to Refs.

18,26, and 22. Our data reflect that this enhancement is then progressively suppressed with increasing confinement, as predicted by either Kinaret and Lee[16] or Balev and Vasilopoulos[17] for high perpendicular magnetic fields. In particular, in the Kinaret and Lee model, the suppression occurs as the magnetic field becomes smaller than a certain critical value B_{cr}, which increases with increasing confinement. At the opposite limit of very high fields $\omega_c/\omega_0 \gg 1$, Balev and Vasilopoulos[17] predict final stability of the spin split phase with increasing field. In qualitative agreement with theory the magnetic fields, at which in our experiments spin splitting is resolved, increase with increasing confinement. While for weak confinement the condition $B > B_{cr}$ for stability of the spin split phase is already fulfilled at 7 T, for stronger confinement it is fulfilled only beyond 10 T. Furthermore, the strong enhancement of the *g*-factor at low values of the side gate voltage suggests that our case is just in the critical region, where the transition into the spin split phase takes place and thus abrupt changes are indeed predicted.[16]

We note that, just for the way capacitance measurements intrinsically works, we are not able to observe directly how the spin gap evolves by changing electron density, leaving all the other parameters unchanged. Indeed, we can only observe spin splitting, if present at all, at the density at which the upper spin split level starts to be filled. Nevertheless, we can study the spin gap at different densities via changing either confinement or magnetic field. Yet, as both the actual density and the critical density are changed by magnetic field and confinement, the interpretation of our data requires simultaneous comparison of a whole set of measurements.

Unfortunately, in our sample we miss the crossover between the purely 2D regime, with *g* factor typically ranging between 3 and 7, and the 1D one, with enhanced *g* factor. We would expect to see the *g* factor first to increase with increasing confinement, reach a maximum, and then decrease. Only the latter regime is in fact observed in our data. Our limit is due to surface charges, which cause a modulation of the potential even at zero side gate voltage and thus make the side gate voltage practically ineffective in the regime of very low confinements.

IV. CONCLUSIONS

In this paper, we describe magnetocapacitance traces measured on arrays of quantum wires induced by field effect in MIS-type GaAs/AlGaAs heterostructures. By means of interlocked central and side gate, we are able to control one-dimensional confinement and electron density down to the quantum limit, i.e., only the first subband occupied. We explore band filling and energy levels spacing as a function of confining voltage and magnetic field. Our data are very well reproduced by a simple analytical model, whose validity is *a posteriori* demonstrated by comparison with self-consistent two-dimensional Poisson-Schrödinger simulations. A qualitative explanation for the evolution of the shape of capacitance traces in terms of changes in the DOS is given. We analyze the behavior of spin splitting and explain it within the framework of existing theories. As a result of the competition between exchange interactions and kinetic contribution from edge states, the spin gap at low confinement is enhanced with respect to the two-dimensional case, but it is monotonously suppressed with increasing confinement in the range $\hbar\omega_0 \approx 4.5-7$ meV. Only at very strong magnetic field $B > 10$ T the spin splitting is still visible at the highest confinement investigated. We extract the corresponding *g* factor, which turns out to be at 14 T as high as $g \approx 21$ at the lowest confinement and $g \approx 4$ at the largest confinement.

ACKNOWLEDGMENTS

This work was financially supported by DFG via SFB508 ''Quantum materials'' and by the European Union via the TMR program. The authors gratefully thank D. Schmerek, who developed the Schrödinger-Poisson calculation, as well as S. Schnüll, C. Weichsel, and D. Schuster for technical assistance.

*Electronic address: pallecc@fisica.unige.it

[1] F. F. Fang and P. J. Stiles, Phys. Rev. **174**, 823 (1968).
[2] J. F. Janak, Phys. Rev. **178**, 1416 (1969).
[3] T. Ando and Y. Uemura, J. Phys. Soc. Jpn. **37**, 1044 (1974).
[4] R. J. Nicholas, R. J. Haug, K. v. Klitzing, and G. Weimann, Phys. Rev. B **37**, 1294 (1988).
[5] A. Usher, R. J. Nicholas, J. J. Harris, and C. T. Foxon, Phys. Rev. B **41**, 1129 (1990).
[6] A. Pinczuk, B. S. Dennis, D. Heiman, C. Kallin, L. Brey, C. Tejedor, S. Schmitt-Rink, L. N. Pfeiffer, and K. W. West, Phys. Rev. Lett. **68**, 3623 (1992).
[7] S. A. J. Wiegers, M. Specht, L. P. Lvy, M. Y. Simmons, D. A. Ritchie, A. Cavanna, B. Etienne, G. Martinez, and P. Wyder, Phys. Rev. Lett. **79**, 3238 (1997).
[8] V. T. Dolgopolov, A. A. Shashkin, A. V. Aristov, D. Schmerek, W. Hansen, J. P. Kotthaus, and M. Holland, Phys. Rev. Lett. **79**, 729 (1997).
[9] B. B. Goldberg, D. Heiman, and A. Pinczuk, Phys. Rev. Lett. **63**, 1102 (1989).
[10] C. Hermann and C. Weisbuch, Phys. Rev. B **15**, 823 (1977).
[11] M. Dobers, K. v. Klitzing, and G. Weimann, Phys. Rev. B **38**, 5453 (1988).
[12] D. Stein, K. v. Klitzing, and G. Weimann, Phys. Rev. Lett. **51**, 130 (1983).
[13] S. L. Sondhi, A. Karlhede, S. A. Kivelson, and E. H. Rezayi, Phys. Rev. B **47**, 16 419 (1993).
[14] S. E. Barrett, G. Dabbagh, L. N. Pfeiffer, K. W. West, and R. Tycko, Phys. Rev. Lett. **74**, 5112 (1995).
[15] A. Schmeller, J. P. Eisenstein, L. N. Pfeiffer, and K. W. West, Phys. Rev. Lett. **75**, 4290 (1995).
[16] J. M. Kinaret and P. A. Lee, Phys. Rev. B **42**, 11 768 (1990).
[17] O. G. Balev and P. Vasilopoulos, Phys. Rev. B **56**, 6748 (1997).
[18] K. Shepard, Phys. Rev. B **45**, 13 431 (1992).
[19] J. Wróbel, F. Kuchar, K. Ismail, K. Y. Lee, H. Nickel, W. Schlapp, G. Grabecki, and T. Dietl, Surf. Sci. **305**, 615 (1994).
[20] M. A. Kastner, S. B. Field, J. C. Licini, and S. L. Park, Phys. Rev. Lett. **60**, 2535 (1988).
[21] R. Mottahedeh, M. Pepper, R. Newbury, J. A. A. J. Perenboom, and K. F. Berggren, Solid State Commun. **72**, 1065 (1989).
[22] R. Kotlyar, L. Reinecke, M. Bayer, and A. Forchel, Phys. Rev. B **63**, 085310 (2001).

[23] K. J. Thomas, M. Y. Simmons, J. T. Nicholls, D. R. Mace, M. Pepper, and D. A. Ritchie, Appl. Phys. Lett. **67**, 109 (1995).
[24] K. J. Thomas, J. T. Nicholls, M. Y. Simmons, M. Pepper, D. R. Mace, and D. A. Ritchie, Phys. Rev. Lett. **77**, 135 (1996).
[25] K. S. Pyshkin, C. J. B. Ford, R. H. Harrell, M. Pepper, E. H. Linfield, and D. A. Ritchie, Phys. Rev. B **62**, 15 842 (2000).
[26] A. Gold and A. Ghazali, Phys. Rev. B **41**, 8318 (1990).
[27] A. Majumdar, J. Appl. Phys. **83**, 297 (1998).
[28] C. K. Wang and K. F. Berggren, Phys. Rev. B **54**, 14 257 (1996).
[29] K. J. Thomas, J. T. Nicholls, N. J. Appleyard, M. Y. Simmons, M. Pepper, D. R. Mace, W. R. Tribe, and D. A. Ritchie, Phys. Rev. B **58**, 4846 (1998).
[30] A. J. Daneshvar, C. J. B. Ford, A. R. Hamilton, M. Y. Simmons, M. Pepper, and D. A. Ritchie, Phys. Rev. B **55**, R13 409 (1997).
[31] T. P. Smith, J. A. Brum, J. M. Hong, C. M. Knoedler, and H. Arnot, Phys. Rev. Lett. **61**, 585 (1988).
[32] D. Schmerek and W. Hansen, Phys. Rev. B **60**, 4485 (1999).
[33] H. Drexler, W. Hansen, S. Manus, J. P. Kotthaus, M. Holland, and P. Beaumont, Phys. Rev. B **49**, 14 074 (1994).
[34] D. Schmerek and W. Hansen, Physica E (Amsterdam) **6**, 547 (2000).
[35] B. Kardynal, C. H. W. Barnes, E. H. Linfield, D. A. Ritchie, J. T. Nicholls, K. M. Brown, G. A. C. Jones, and M. Pepper, Phys. Rev. B **55**, R1966 (1997).
[36] S. E. Laux, D. J. Frank, and F. Stern, Surf. Sci. **196**, 101 (1988).
[37] D. Schmerek, S. Manus, A. O. Govorov, W. Hansen, and J. P. Kotthaus, Phys. Rev. B **54**, 13 816 (1996).